NASA/TM–2007–214855

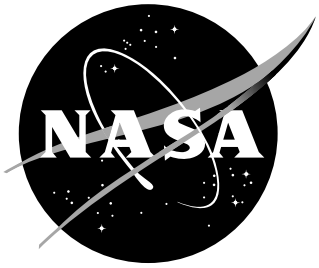

An Investigation of Synchrony in Transport Networks

Rex K. Kincaid
College of William & Mary, Williamsburg, Virginia

Natalia M. Alexandrov
NASA Langley Research Center, Hampton, Virginia

Michael J. Holroyd
University of Virginia, Charlottesville, Virginia

March 2007

Since its founding, NASA has been dedicated to the advancement of aeronautics and space science. The NASA Scientific and Technical Information (STI) Program Office plays a key part in helping NASA maintain this important role.

The NASA STI Program Office is operated by Langley Research Center, the lead center for NASA's scientific and technical information. The NASA STI Program Office provides access to the NASA STI Database, the largest collection of aeronautical and space science STI in the world. The Program Office is also NASA's institutional mechanism for disseminating the results of its research and development activities. These results are published by NASA in the NASA STI Report Series, which includes the following report types:

- TECHNICAL PUBLICATION. Reports of completed research or a major significant phase of research that present the results of NASA programs and include extensive data or theoretical analysis. Includes compilations of significant scientific and technical data and information deemed to be of continuing reference value. NASA counterpart of peer-reviewed formal professional papers, but having less stringent limitations on manuscript length and extent of graphic presentations.
- TECHNICAL MEMORANDUM. Scientific and technical findings that are preliminary or of specialized interest, e.g., quick release reports, working papers, and bibliographies that contain minimal annotation. Does not contain extensive analysis.
- CONTRACTOR REPORT. Scientific and technical findings by NASA-sponsored contractors and grantees.
- CONFERENCE PUBLICATION. Collected papers from scientific and technical conferences, symposia, seminars, or other meetings sponsored or co-sponsored by NASA.
- SPECIAL PUBLICATION. Scientific, technical, or historical information from NASA programs, projects, and missions, often concerned with subjects having substantial public interest.
- TECHNICAL TRANSLATION. English-language translations of foreign scientific and technical material pertinent to NASA's mission.

Specialized services that complement the STI Program Office's diverse offerings include creating custom thesauri, building customized databases, organizing and publishing research results ... even providing videos.

For more information about the NASA STI Program Office, see the following:

- Access the NASA STI Program Home Page at ***http://www.sti.nasa.gov***
- E-mail your question via the Internet to help@sti.nasa.gov
- Fax your question to the NASA STI Help Desk at (301) 621–0134
- Phone the NASA STI Help Desk at (301) 621–0390
- Write to:
  NASA STI Help Desk
  NASA Center for AeroSpace Information
  7115 Standard Drive
  Hanover, MD 21076–1320

NASA/TM–2007–214855

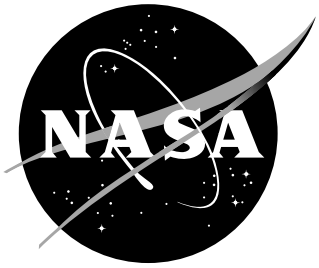

An Investigation of Synchrony in Transport Networks

Rex K. Kincaid
College of William & Mary, Williamsburg, Virginia

Natalia M. Alexandrov
NASA Langley Research Center, Hampton, Virginia

Michael J. Holroyd
University of Virginia, Charlottesville, Virginia

National Aeronautics and
Space Administration

Langley Research Center
Hampton, Virginia 23681-2199

March 2007

Acknowledgments

The authors would like to thank the NASA Aeronautics Research Directorate for funding this work during the summer of 2006 via the NASA Faculty Fellowship Program. This work was also partially supported by the NASA Grant NNL05AA30G and the Faculty Research Award from the College of William & Mary. The authors would like to thank the Aeronautics Systems Analysis Branch of the NASA Langley Systems Analysis and Concepts Directorate for providing an environment for this collaboration.

Available from:

NASA Center for AeroSpace Information (CASI)
7115 Standard Drive
Hanover, MD 21076–1320
(301) 621–0390

National Technical Information Service (NTIS)
5285 Port Royal Road
Springfield, VA 22161–2171
(703) 605–6000

Abstract

The cumulative degree distributions of transport networks, such as air transportation networks and respiratory neuronal networks, follow power laws. The significance of power laws with respect to other network performance measures, such as throughput and synchronization, remains an open question. Evolving methods for the analysis and design of air transportation networks must be able to address network performance in the face of increasing demands and the need to contain and control local network disturbances, such as congestion. Toward this end, we investigate functional relationships that govern the performance of transport networks; for example, the links between the first nontrivial eigenvalue, λ_2, of a network's Laplacian matrix—a quantitative measure of network synchronizability—and other global network parameters. In particular, among networks with a fixed degree distribution and fixed network assortativity (a measure of a network's preference to attach nodes based on a similarity or difference), those with small λ_2 are shown to be poor synchronizers, to have much longer shortest paths and to have greater clustering in comparison to those with large λ_2. A simulation of a respiratory network adds data to our investigation. This study is a beginning step in developing metrics and design variables for the analysis and active design of air transport networks.

1 Introduction

The U.S. and world-wide air transport networks are *scale-free*[1], i.e., their degree distributions follow power laws [9, 10]. A large body of recent work has been published on scale-free networks including the popular books *Linked* by Barabási [4] and *Six Degrees* by Watts [21]. A number of excellent review articles, including Newman [17], Strogatz [19], Albert and Barabási [1] and Dorogovtsev and Mendes [6], contain hundreds of references.

Arguably, many scale-free networks occurring in natural and technological realms have never been actively designed in the traditional sense: identify design variables, objectives, and constraints and follow a prescriptive algorithm to obtain a design that satisfies constraints and is "optimal" with respect to the given objectives. Rather, these networks have evolved in response to demands, in accordance with some natural or technological rules. Thus many of the investigations have been of an analytical nature, i.e., given a particular natural or technological network, its characteristics are studied. Our ultimate interest is to take a step from analysis to active design and our motivation comes from air transport systems. We emphasize that complex networks will likely never be completely amenable to traditional design methods, given the intrinsic lack of predictive modeling akin to that of physical artifacts (e.g., airplanes, automobiles). However, we conjecture that some measure of active design is still possible with the identification of appropriate design variables and metrics. Specifically, we are looking for an appropriate functional relation between global metrics (e.g., throughput, delays, capacity, synchronizability) and locally controllable structure (e.g., connectivity, degree).

Air transport networks are our ultimate domain of interest. Are scale-free networks desirable for air transport? Given a fixed degree distribution, how should the network links be configured to achieve optimal performance for relevant metrics? Can salient features of scale-free air transport networks critical to network performance be identified?

With the advent of deregulation of the U.S. air transport system in 1978, airlines began to organize their operations with a *hub-and-spoke* approach. Two natural outcomes have been an increase in flight frequency and an increase in the variance of flight times. Recently,

[1] We use the term "scale-free" here to denote networks whose degree distributions follow a power law. Due to a wide range of properties possessed by networks of similar degree distributions, there is an ongoing discussion of the meaning of "scale-free" [13].

competitors to the hub-and-spoke model have garnered attention with the use of *point-to-point* flight schedules. With the delays experienced by travelers at hub airports these direct flights are an attractive alternative. How will these point-to-point airlines alter the air transport network structure? Can we provide any guidance to local air routing decisions with global air transport network performance measures in mind? To begin to address these questions we examine the effects of a network metric for synchronization on transport route structure by holding the degree distribution and a scale-free/scale-rich metric constant. We also report on a simulation of a respiratory neuronal network used as an additional testbed for investigating the synchrony metrics. It is a first step in the investigation aimed at deriving the functional dependences among various local network properties and the aggregated metrics of interest to participants in the transportation system in an effort to eventually arrive at active transport network design and optimization algorithms.

2 Background

In this section we briefly review some of the network attributes salient to our investigation into the network functional relationships. Early network growth models were based on preferential attachment. A variety of authors have developed extensions and improvements to the early models. All of these mechanisms build networks sequentially, one node at a time. Barabasi's [4] original approach selected the end nodes for the edges associated with the new node based solely on the current network's degree distribution. Subsequent efforts have altered the end node selection method to control other network features. For example, Wang *et al.* [20] develop a growth model in which *assortativity* is tunable while Schank and Wagner [18] and Holme and Kim [11] grow networks with tunable clustering coefficients.

The network attribute under study here is synchronicity. One notion of synchronicity has to do with the network's tendency to synchronize over time, given a specific static structure of the network. In particular, we are not yet considering explicit traffic flows through the air transport network. Instead, we are investigating how the node (e.g., airport) connectivity may influence the traffic flow.

Of importance here is the *tunability* of a given network with respect to synchronicity. We realize tunability as network optimization. Before proceeding further we provide a definition of network synchronization for a discrete complex system. Given a connected network, denote the state of a node i at time t by $x_i(t)$. How do the states of the nodes change over time? Clearly if nodes do not rely on any information generated by adjacent nodes then there is no opportunity of synchronization. Atay *et al.* [2, 3] assume that all nodes are identical and conform to the following generic discrete time equation to determine their next state:

$$x_i(t+1) = f(x_i(t)) + \kappa \left[\frac{1}{k_i} \sum_{j|(i,j)\in Edges} f(x_j(t)) - f(x_i(t)) \right], \tag{1}$$

where κ, known as the *coupling constant*, is a scalar describing the extent to which neighbors effect the state of a node; $f(\cdot)$ is any differentiable function mapping some finite interval to itself. The function $f(\cdot)$ describes the behavior of a node in the absence of any outside influence. We say that a network *synchronizes* for a given initial condition if for all i, j

$$\lim_{t\to\infty} |x_i(t) - x_j(t)| = 0. \tag{2}$$

Note that if $\kappa = 0$, then the equation becomes $x_i(t+1) = f(x_i(t))$.

One attribute that correlates with the network's capacity to synchronize is the first nontrivial eigenvalue, λ_2, of the Laplacian matrix associated with the network structure

(more about λ_2 in the next section). Here λ_2 acts as a measure of the range of κ over which the network will synchronize.

Clearly, air transport networks will not meet some of the assumptions. The nodes (airports) are not all identical and we are more interested in the transient (say, 24 hour period) behavior than in what happens as $t \to \infty$. Nonetheless, in the next section we will see that λ_2 will provide useful information with regard to network structure and synchrony.

For some complex systems synchronization is an essential feature. For example, in mammals a small group of neurons (roughly 200) is responsible for generating a regular rhythmic output to motor cells that initiate a breath. (We explore this example further in Section IV.) Without synchronization of the neuronal output, breathing would be ragged or not occur at all. However, in the defined sense, synchronization is an undesirable attribute for air transport networks. Think of the airports as neurons in our mammalian respiratory example. Inhaling means all planes land at all airports simultaneously. Exhaling means they depart together. The result is congestion. Thus, for the given definition, one would like an air transport network design to minimize synchronization.

Another network metric, developed in [13], serves to classify the ways in which networks with a given degree distribution may be constructed. The metric is $s(G)$, where G stands for "graph" (networks and graphs are interchangeable). To determine $s(G)$, compute the product of the degrees of the end nodes for each edge or link, sum them up for all edges, and divide by s_{max}, where s_{max} is the maximum value of the sum taken over all possible connected graphs for a fixed degree distribution. That is,

$$s(G) = (\sum_{(i,j)\in Edges)} d_i \times d_j)/s_{max}, \tag{3}$$

where d_i is the degree of node i. The value of s_{max} provides a way to scale the sum of the product of the degrees for each edge. In [13], for a fixed degree distribution, graph realizations with large values of $s(G)$ are termed *scale-free* and graph realizations with small values of $s(G)$ are termed *scale-rich*. Consequently, scale-free graphs or networks are those in which high degree nodes are more likely to be adjacent to other high degree nodes while scale-rich graphs are those for which high degree nodes are more likely to be adjacent to low degree nodes. As shown in [13], $s(G)$ and assortativity are equivalent but are scaled in different ways. Typically the scaling for the assortativity measure leads to a tighter range of values for a given degree distribution. For further information about $s(G)$ and how it is used to distinguish between networks for the Internet at the router level the interested reader is referred to [13] and [14].

	Internet	**Air Transport**
product	packets	planes (loaded)
constraint	bandwidth	airport capacity
competitors	ISPs	airlines
links	hardwired	FAA/Airlines
distributors	routers	airports

Table 1. Analogy between Internet router and air transport networks.

The problems faced by designers of air transport networks share some aspects with the design of an Internet router network. Many authors have contributed to investigations of how a router network is constructed. Two references in this field, [13] and [14], contain ideas central to our consideration of the design of air transport networks. At one level of resolution, Table 1 points out the analogies between these two network design problems. With regard to bandwidth, the Internet router designer must weigh the trade-offs between

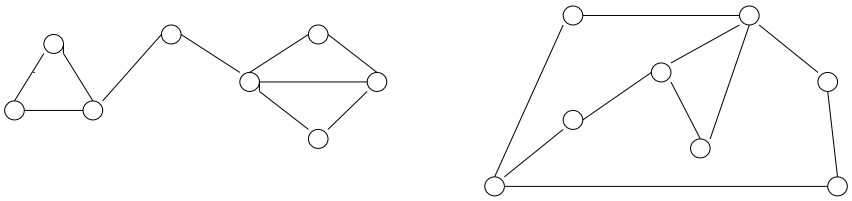

Figure 1. Geometric graph with $\lambda_2 = 0.238$ and $\lambda_2 = 0.925$

many low bandwidth connections and fewer high bandwidth connections. These trade-offs are akin to choosing between a few hub airports in a hub-and-spoke system and choosing lower frequency airports that might arise in a direct route system. Of course, there are many differences as well. The variation in the size of the packets for the Internet is not nearly as great as the number of passengers on planes of different sizes. In addition, although the FAA[2] clearly defines the routes allowed between airports, the links are as not hard-wired as they are in the Internet model. Still there is much to be learned from the research efforts on the design of effective Internet router networks.

3 Network Experiments with λ_2

In this section the interplay between λ_2, a gross measure of network synchrony, and $s(G)$, a network measure similar to assortativity is examined. Networks of two types—preferential attachment and geometric—are the testbeds. Each network has 100 nodes and is a simple undirected network (no self-loops, no multiple edges). An adjacency matrix, A, is constructed. $G(V, E)$ denotes a graph (network) with vertex (node) set V and edge (link) set E. For each network type the degree distribution and $s(G)$ values are fixed. Finally, a tabu search heuristic rewires a given network so as to minimize (or maximize) the value of λ_2.

Preferential attachment graphs are generated following the approach given in [4]. The network is grown by adding nodes and edges. For each node added, m edges are added preferentially, based on the current degree distribution. Geometric graphs are generated by randomly selecting 100 points (r, θ) with values of $r \in [0, 1]$ and values of $\theta \in (0, 360]$. Edges exist between pairs of points if the Euclidean distance is less than a specified threshold (in our experiments thresholds between 0.17 and 0.25 were used). If the resulting graph is connected, it is kept; otherwise it is rejected and the process begins again. A variety of network performance measures are available. These include network diameter, average degree, assortativity, clustering coefficient, synchrony and $s(G)$.

Our measure of synchrony relies on computing an eigenvalue of the Laplacian matrix associated with a given network structure. For our networks or graphs the Laplacian matrix is a symmetric matrix $L = D - A$, where D is a diagonal matrix with the degree of each node located along the main diagonal. A is the adjacency matrix for the graph. The second eigenvalue of L measures algebraic connectivity [7]. Intuitively, graphs with small λ_2 are easier to "pull apart". In particular, if $\lambda_2 = 0$, then the graph is disconnected. Many authors [2, 5, 22] have convincingly used λ_2 as a global measure of how likely a graph is to synchronize. That is, given an arbitrary flow of entities, the graph is less likely to synchronize if λ_2 is small. The two graphs in Figure 1 have identical degree distributions, but the graph on the left is more weakly connected (e.g., the removal a single edge can disconnect the graph). The identification of structural differences between large graphs

[2] Federal Aviation Administration

with varying values of λ_2 is studied in the following set of numerical experiments.

In the remainder of the section, we describe numerical experiments in optimizing two types of networks for λ_2: geometric graphs with 100 nodes and preferential attachment graphs with $m = 2$.

The graphs plotted in Figures 2 and 3 were constructed by first generating a random instance of the particular graph class—geometric in Figure 2 or preferential attachment in Figure 3. Next, a simple tabu search [8] heuristic was called to minimize or maximize λ_2 while keeping the degree distribution and $s(G)$ fixed. Allowable moves (re-wirings) are pair-wise edge interchanges that preserve the degree distribution and $s(G)$. Briefly, the tabu search checks to see if the move is acceptable, that is, if the move is improving and not tabu, or improving and tabu but leads to the best observed value of λ_2 (aspiration criterion). Note that these moves are precisely the moves allowed in a random rewiring scheme without checking for the preservation of $s(G)$. The interested reader is referred to Glover and Laguna [8] for further information on tabu search.

Figures 2-4 display networks with respect to the reciprocal of the eccentricity of each node u. The eccentricity of u is its maximum (shortest path) distance. The graphs are generated by `socnetv`[3]. The goal of the plots is to uncover any qualitative differences between the graphs with small and large values of the second eigenvalue of the Laplacian.[4] For each pair of plots in a figure, the number of nodes (100), the degree distribution, and the value of $s(G)$ is fixed.

Nodes with equal eccentricity values are plotted on the same (dashed line) circles. The circles with larger radii have larger eccentricity. Consequently, nodes near the center have shorter longest paths. The paired plots exhibit large qualitative differences in the eccentricity patterns. The same pairs of plots for other available measures in `socnetv` were also constructed. Although small variations were seen, none of the other paired plots exhibited significant differences.

Qualitatively, when λ_2 is small, the patterns are less organized, the eccentricity plots in Figures 2a and 3a are more dispersed and consist of many rings of constant eccentricity. The eccentricity plots with larger λ_2 are more organized, with few rings of constant eccentricity. Specifically, the plots with small λ_2 have 11 (Figure 2a) and 10 (Figure 3a) rings. For larger λ_2 there are five (Figure 2b) and four (Figure 3b) rings, respectively. The ranges of eccentricity values for the small λ_2 plots are dominated by the ranges for the large λ_2 plots. For example, the range of eccentricity values for the geometric graph with small λ_2 (Figure 2a) is $[26, 42]$ and for the geometric graph with large λ_2 (Figure 2b) it is $[4, 8]$. Thus, the patterns of eccentricities in Figures 2b-3b are non-overlapping and dominate those given in Figures 2a-3a.

The diameter of the graph in Figure 2a is 42 while the graph diameter in Figure 2b is 8. The diameters are 19 and 6 for graphs in Figure 3. Notice that this is also true for the simple graphs in Figure 1. The graph on the left has a larger diameter than the one on the right. For graphs with a fixed degree distribution and a fixed value of $s(G)$, this result appears to hold in general. We know of no theorem that proves this result but numerous computational tests support this claim so far. Moreover, the inverse relationship between λ_2 and the eccentricity does not hold if $s(G)$ is allowed to vary. Figures 4a and 4b provide an example. The value of $\lambda_2 = 0.935$ in Figure 4a is larger than $\lambda_2 = 0.440$ in Figure 4b. Yet the range of eccentricity values for Figure 4a, $[8, 16]$, is larger and does not overlap with the range for Figure 4b of $[3, 6]$.

In Figures 5 and 6, we investigate the relation between $s(G)$ and the clustering coefficient, $c(G)$ [17], of a network or graph. These figures display results for 5000 geometric graphs. In Figure 5, the 5000 geometric graphs are generated randomly. Edges connect nodes if the

[3]The source code and documentation can be found at `http://socnetv.sourceforge.net/`.

[4]We leave it to the reader to become acquainted the variety of measures and display features in `socnetv`. For the purposes of this exposition, we are interested only in the qualitative differences between the plots.

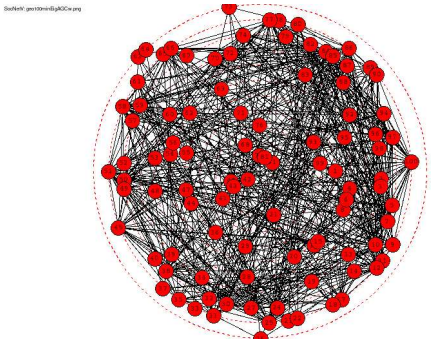

(a) $\lambda_2 = 0.009$, $e(V) = (26, 42)$, $c(G) = 0.426$

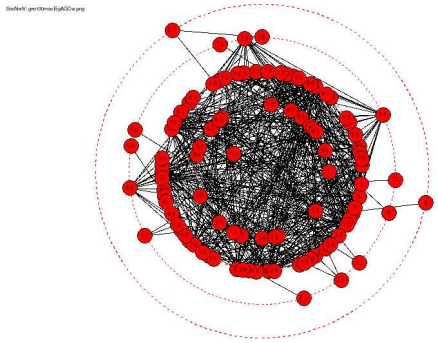

(b) $\lambda_2 = 0.314$, $e(V) = (4, 8)$, $c(G) = 0.297$

Figure 2. Geometric graphs: 100 nodes, $s(G) = 0.971$, fixed degree distribution

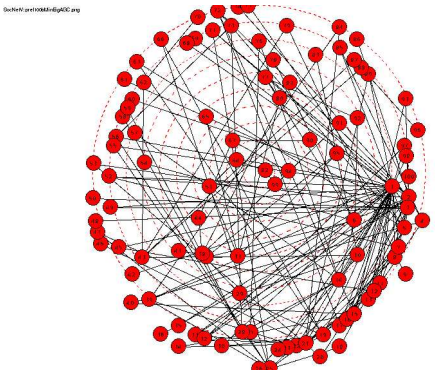

(a) $\lambda_2 = 0.006$, $e(V) = (10, 19)$, $c(G) = 0.210$

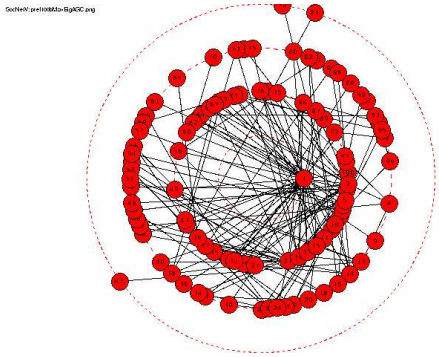

(b) $\lambda_2 = 0.365$, $e(V) = (3, 6)$, $c(G) = 0.101$

Figure 3. Preferential attachment: 100 nodes, $s(G) = 0.716$, fixed degree distribution

Euclidean distance between these nodes is less than 0.23. If the resulting graph is connected, it is kept; otherwise it is rejected and the process begins again. Figure 5b displays the values of $s(G)$ versus $c(G)$. There is no apparent correlation. Figure 6a records the values of $s(G)$ when a given 100-node geometric graph is randomly rewired 5000 times. Figure 6b illustrates the inverse relationship between $s(G)$ and $c(G)$ when the first 364 re-wirings are excluded.

In addition to the inverse relationship between λ_2 and the eccentricity, the clustering coefficient varies inversely with λ_2 in Figures 2 and 3. Notice that when $s(G)$ is not held constant, as in Figure 4, this relationship does not hold. A similar trend between $s(G)$ and $c(G)$ is observed in Figure 6. Figure 6a displays the value of $s(G)$ versus 5000 random re-wirings of a given geometric graph. We note that the same moves as those used in our tabu search to optimize λ_2 are used for the random re-wirings. Figure 6b plots $s(G)$ versus $c(G)$ for the last 4634 random re-wirings and $s(G)$ varies inversely with $c(G)$. Notice that in Figure 6a, the first 600 or so random re-wirings decrease $s(G)$ almost monotonically before settling into an oscillating pattern of increases and decreases in the range of $(0.79, 0.83)$. This is not the case, however, when geometric graphs are generated at random (no rewiring), as in Figure 5. Here no correlation is exhibited between $c(G)$ and $s(G)$.

As we have noted earlier, Figures 4a-b illustrate that $s(G)$, or some yet unknown network metric, appears to exert significant influence on the eccentricity pattern. In Figure 2b,

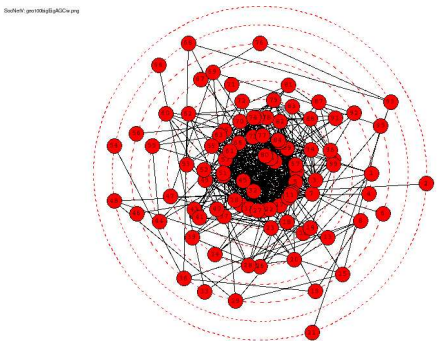

(a) $\lambda_2 = 0.935$, $s(G) = 0.797$, $e(V) = (8, 16)$, $c(G) = 0.306$

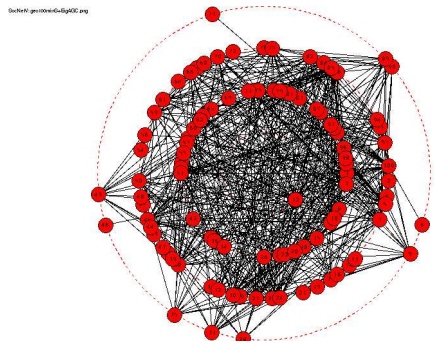

(b) $\lambda_2 = 0.440$, $s(G) = 0.677$, $e(V) = (3, 6)$, $c(G) = 0.126$

Figure 4. Geometric graphs: 100 nodes, fixed degree distribution, varying $s(G)$

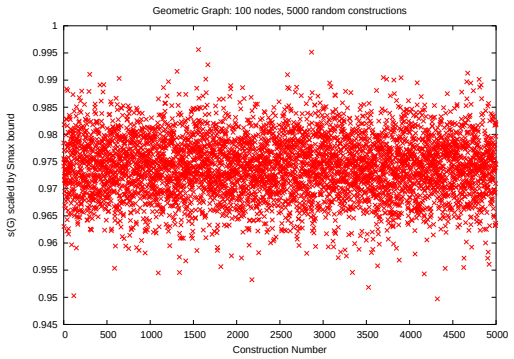

(a) $s(G)$

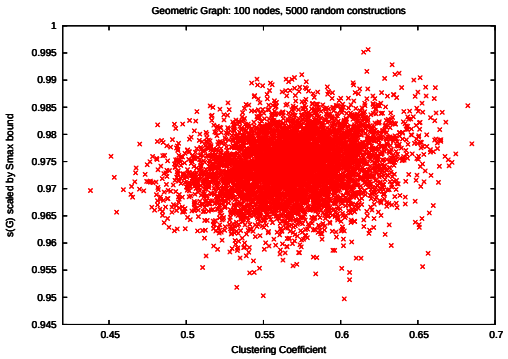

(b) $s(G)$ vs. $c(G)$

Figure 5. 5000 Random geometric graphs

$\lambda_2 = 0.314$, $s(G) = 0.971$, and the eccentricity range is $[4, 8]$. This compares favorably with the results in Figure 4b, where $\lambda_2 = 0.440$ is larger and the eccentricity range of $[3, 6]$ is smaller with a smaller minimum node eccentricity. However, the comparisons with Figure 4a are not consistent. The value for λ_2 in Figure 4a is larger but, unexpectedly, the max and min values for the eccentricity range are much larger than those in Figure 2b. In addition, the previously observed pattern of $c(G)$ varying inversely with λ_2 no longer holds. For example, λ_2 decreases from 0.935 in Figure 4a to 0.440 in Figure 4b. Similar decreases observed in Figures 2 and 3 led to a doubling of $c(G)$. But here $c(G)$ decreases by more than a half. It is unclear if the role of $s(G)$ explains the lack of consistency. Figure 5 provides one possible explanation. Here geometric graphs are generated at random (no rewiring) and there is no correlation between $s(G)$ and $c(G)$. In Figure 6, an inverse correlation exists but here the graphs are constructed by successively rewiring a single geometric graph at random.

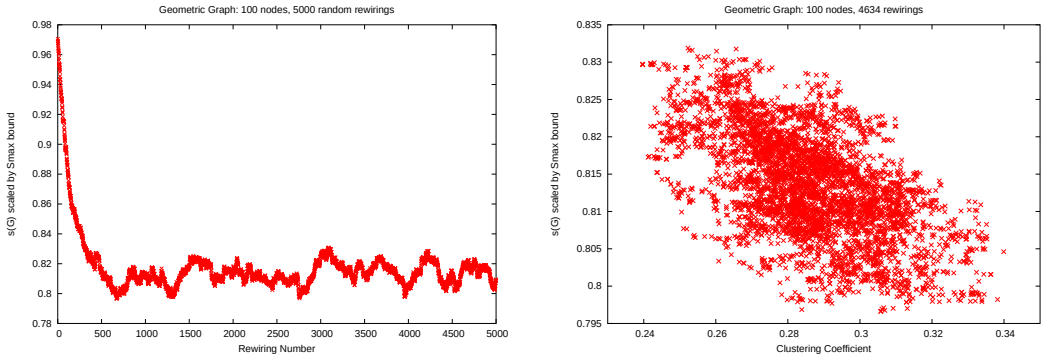

(a) $s(G)$ (b) $s(G)$ vs. $c(G)$

Figure 6. 5000 Re-wirings of a Geometric Graphs

4 Respiratory Network Simulation

In the previous section we have seen that when the degree distribution and $s(G)$ are fixed, there is a predictable difference in the shortest path distribution (eccentricity measures) and the clustering coefficients. Ideally the next step would be to simulate the performance of networks presented in the previous section and investigate their performance as air transport network systems. We are currently proceeding in this direction using a model previously developed to simulate the complete U.S. air transport system. For now, we provide simulation results for a different system—a respiratory neural network—for which a simpler simulation model was readily available. In this model, synchronization (rhythmic breathing) is desired.

Although synchronization is undesirable for air transport networks, there are systems for which it is an essential feature. In mammals, a small group of neurons is responsible for generating a regular rhythmic output to motor cells that initiate a breath. The network structure of these neurons allows them to synchronize without any external influence and produce regular bursts that lead to breaths. In [12], two geometric networks, one with a value of $\lambda_2 = 0.025$ and a second with a value of $\lambda_2 = 0.974$ were tested in a simulation model [16] of this neuronal network. The rhythmic output from the the network with $\lambda_2 = 0.025$ was ragged with fuzzy bursts, while outputs from the network with $\lambda_2 = 0.974$ was sharp with clear, regular bursts (Figure 7).

In mammals, a small group of neurons in the brain stem, called the pre-Bötzinger complex, is responsible for generating a regular rhythmic output to motor cells that initiate a breath. Disconnected, these neurons are unable to provide sufficient output to activate the motor neurons, but their interconnected network structure allows them to synchronize without any external influence and produce regular bursts. Using a detailed simulation due by Hayes [16], we were able to experiment with how different network topologies control the effectiveness of the pre-Bötzinger complex. We began by testing two geometric graphs with extreme values of λ_2. The results of the two simulations, depicted in Figure 7, provide compelling evidence for the utility of λ_2 as a predictor of synchronization. It is easy to see that the network with higher λ_2 synchronizes more strongly than the other network. The second set of simulations investigated two preferential attachment networks. The raster plots in Figure 8 are nearly indistinguishable. The results of the simulation are further analyzed via an autocorrelation analysis (Figure 8). Analysis (as in [16]) uncovers better synchronization in the network with the higher value of λ_2. The results in Figure 9 confirm that, although the difference is undetectable at a first glance (Figure 8), higher λ_2 results in

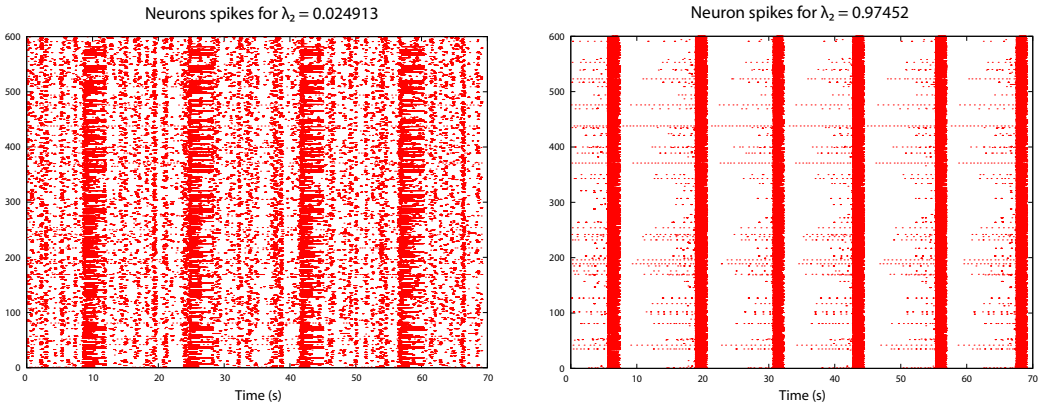

Figure 7. Raster plots of neuron output for two networks with disparate λ_2 values. A point at (x, y) indicates neuron x is spiking at time y. The higher λ_2 network displays much stronger synchronization among all nodes as predicted, as well as a quicker breath frequency.

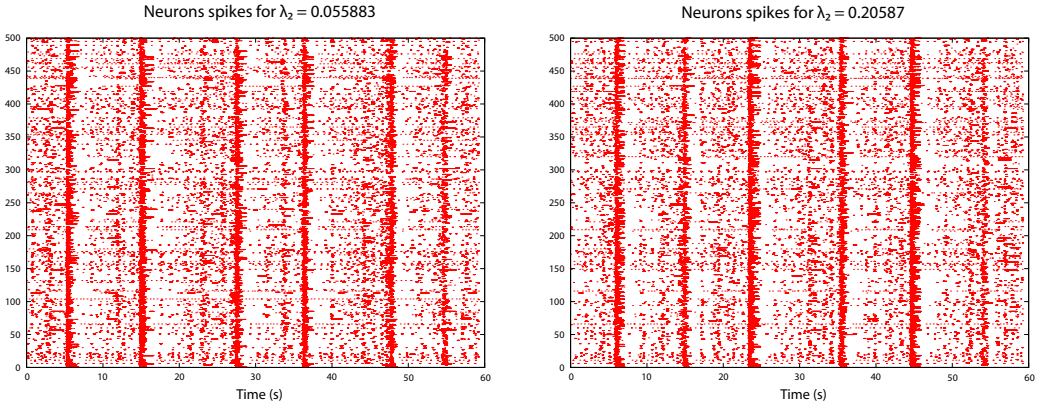

Figure 8. Indistinguishable raster plots of simulated neuron output for two sample networks with differing λ_2 values.

a better synchronization. Autocorrelation indicates the largest difference during the refractory (non-spiking) period: the two graphs exhibit similar behaviors during spikes, but not between spikes. These experiments provide further evidence that λ_2 can be used to identify graphs (networks) that are not likely to synchronize.

5 Conclusions and Discussion

Given the present state of air transportation networks, there is some urgency in developing active and rigorous design methodologies. Our goal is to develop a systematic way to design for some salient aspects of air transport networks. In particular, network structure, both static (node location) and dynamic (air route scheduling) has a direct effect on the functioning of the traffic in the network; we are now concerned with the effect of the static and dynamic network structure on the performance.

How should the design process proceed? Design involves being able to manipulate variables so as to optimize objectives subject to constraints. As a step in this direction we have

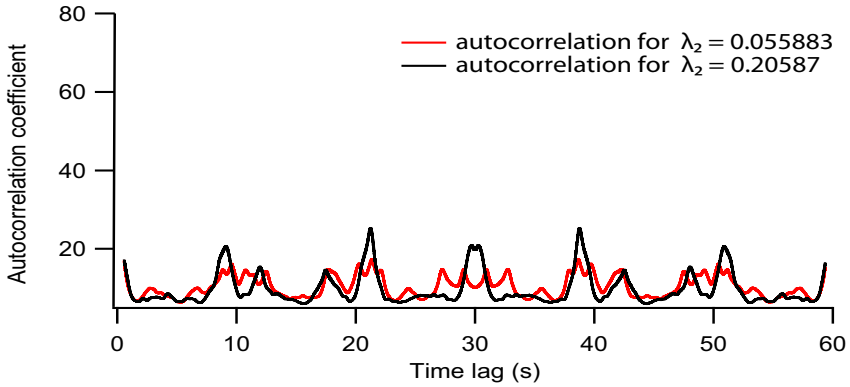

Figure 9. An autocorrelation plot of pre-Bötzinger complex synchronization on two networks with the same degree distribution, but with differing λ_2 values. The autocorrelation analysis shows that the higher λ_2 network displays better synchronization.

demonstrated that for a fixed degree distribution and fixed $s(G)$ value (and, consequently, a fixed assortativity), optimizing for λ_2 yields networks with distinct eccentricity patterns. We have demonstrated the ability to construct networks with locally optimal λ_2 and observed a correlation with global network attributes, such as clustering, eccentricity and synchronizability. These results are further supported by a simulation analysis of another transport system – a respiratory neuronal network. This simulation supports our conjecture that large differences in λ_2 result in observable differences in the burst activity: good synchronization for large λ_2 and poor synchronization for small λ_2. It remains to simulate air transport networks with small and large values of λ_2 (more than likely with identical degree distributions and $s(G)$ values). In addition to validating the static results for networks (as in Figures 2 and 3) the simulation will also measure quantities of interest to the FAA that are currently not amenable to rigorous optimization. For example, the simulation will measure congestion effects in air traffic sectors. Finally, one of our major tasks is to derive maps between the network metrics we can control and airspace simulations and, ultimately, FAA metrics. We conjecture that deriving the maps will enable active design for a number of objectives and constraints.

References

1. Albert, R. and A.-L. Barabási, "Statistical Mechanics of Complex Networks," *Rev. Modern Physics*, **74**:42-47 (2002).

2. Atay, F. M. and J. Jost, "Delays, Connection Topology, and Synchronization of Coupled Chaotic Maps," *Physical Review Ltrs.*, **92(14)**:144101(4) (2004).

3. Atay, F. M., T. Biyikoglu and J. Jost, "Synchronization of Networks with Prescribed Degree Distributions," `arXiv:nlin.AO/0407024 v2`, May (2005).

4. Barabási, A.-L., Linked: The New Science of Networks, Perseus, Cambridge, MA, 2002

5. Barahona, M. and L. M. Pecora, "Synchronization in Small-World Networks," *Physical Review Letters*, **89**, no. 5 (2002).

6. Dorogovtsev, S.N. and J.F.F. Mendes, "Evolution of Networks," *Advances in Phys.*, **51**:1079-1187 (2002).

7. Fiedler, M., "Algebraic connectivity of graphs," *Czech. Math. Journal*, **23**, 298–305 (1973).

8. Glover, F. and M. Laguna, Tabu Search, Kluwer Academic Publishers, Boston, MA, 1997.

9. Guimera, R., S. Mossa, A. Turtschi and L.A.N. Amaral, "Structure and Efficiency of the World-Wide Airport Network," Preprint 0312535 (2003) available from http://arxiv.org/abs/cond-mat/.

10. Guimera, R. and L.A.N. Amaral, "Modeling the world-wide airport network," *European Physical Journal B*, **38**, 381-385 (2004).

11. Holme, P. and B.J. Kim "Growing Scale-free Networks with Tunable Clustering," *Physical Review E*, **65** (026107) (2002).

12. Holroyd, M. "Synchronizability and Connectivity of Discrete Complex Systems," *Undergraduate Honors Thesis*, Dept. of Mathematics, College of William and Mary, Williamsburg, VA 23187-8795 (2006).

13. Li, L., D. Alderson, R. Tanaka, J.C. Doyle and W. Willinger, "Towards a Theory of Scale-Free Graphs: Definition, Properties, and Implications," Preprint 0501169v1 (2005) available at http://arXiv:cond-mat/.

14. Li, L., D. Alderson, J.C. Doyle and W. Willinger, "A First-Principles Approach to Understanding the Internet's Router-level Topology" *Proc. ACM SIGCOMM* (2004).

15. Milgram, S., *Psych. Today*, **2**:60 (1967).

16. Negro, C. Del, J. Hayes, C. Morgadi-Valle, D.D. Mackay, R.W. Pace, E.A. Crowder, and J.L. Feldman, "Sodium and Calcium Current-mediated Pacemaker Neurons and Respiratory Rhythm Generation," *J. Neuroscience*, **25**:446-53 (Jan. 2005).

17. Newman, M.E.J., "The Structure and Function of Complex Networks," *SIAM Review*, **45**:167-256 (2003).

18. Schank, T. and D. Wagner "Approximating Clustering Coefficient and Transitivity," *J. of Graph Algorithms and Applications*, **9(2)**:265-275 (2005).

19. Strogatz, S.H., "Exploring Complex Networks," *Nature*, **410**:268-276, March (2001).

20. Wang, W-X., B. Hu, B-H. Wang, and G. Yan `arXiv:cond-mat/0505419 v1`, May (2005).

21. Watts, D.J., Six Degrees: The Science of a Connected Age, Norton, New York, 2003.

22. Wu, C.W., "Perturbation of Coupling Matrices and Its Effect on the Synchronizability in Arrays of Coupled Chaotic Systems," Preprint 0307052 (2006) available at http://arXiv/pdf/nlin.CD/.

REPORT DOCUMENTATION PAGE

Form Approved
OMB No. 0704–0188

1. REPORT DATE *(DD-MM-YYYY)*	2. REPORT TYPE	3. DATES COVERED *(From - To)*
01-03-2007	Technical Memorandum	9/2005–10/2006

4. TITLE AND SUBTITLE
An Investigation of Synchrony in Transport Networks

5a. CONTRACT NUMBER

5b. GRANT NUMBER

5c. PROGRAM ELEMENT NUMBER

6. AUTHOR(S)
Rex K. Kincaid
Natalia M. Alexandrov
Michael J. Holroyd

5d. PROJECT NUMBER

5e. TASK NUMBER

5f. WORK UNIT NUMBER

7. PERFORMING ORGANIZATION NAME(S) AND ADDRESS(ES)
NASA Langley Research Center
Hampton, Virginia 23681-2199

8. PERFORMING ORGANIZATION REPORT NUMBER
L–19323

9. SPONSORING/MONITORING AGENCY NAME(S) AND ADDRESS(ES)
National Aeronautics and Space Administration
Washington, DC 20546-0001

10. SPONSOR/MONITOR'S ACRONYM(S)
NASA

11. SPONSOR/MONITOR'S REPORT NUMBER(S)
NASA/TM–2007–214855

12. DISTRIBUTION/AVAILABILITY STATEMENT
Unclassified-Unlimited
Subject Category 66
Availability: NASA CASI (301) 621-0390

13. SUPPLEMENTARY NOTES
An electronic version can be found at http://ntrs.nasa.gov.

14. ABSTRACT

The cumulative degree distributions of transport networks, such as air transportation networks and respiratory neuronal networks, follow power laws. The significance of power laws with respect to other network performance measures, such as throughput and synchronization, remains an open question. Evolving methods for the analysis and design of air transportation networks must be able to address network performance in the face of increasing demands and the need to contain and control local network disturbances, such as congestion. Toward this end, we investigate functional relationships that govern the performance of transport networks; for example, the links between the first nontrivial eigenvalue, λ_2, of a network's Laplacian matrix—a quantitative measure of network synchronizability—and other global network parameters. In particular, among networks with a fixed degree distribution and fixed network assortativity (a measure of a network's preference to attach nodes based on a similarity or difference), those with small λ_2 are shown to be poor synchronizers, to have much longer shortest paths and to have greater clustering in comparison to those with large λ_2. A simulation of a respiratory network adds data to our investigation. This study is a beginning step in developing metrics and design variables for the analysis and active design of air transport networks.

15. SUBJECT TERMS
complex systems, networks, air transportation

16. SECURITY CLASSIFICATION OF:			17. LIMITATION OF ABSTRACT	18. NUMBER OF PAGES	19a. NAME OF RESPONSIBLE PERSON
a. REPORT	b. ABSTRACT	c. THIS PAGE			STI Help Desk (email: help@sti.nasa.gov)
U	U	U	UU	18	19b. TELEPHONE NUMBER *(Include area code)* (301) 621-0390